Received: 3 July 2019 | Revised: 30 October 2019 | Accepted: 31 December 2019

DOI: 10.1111/cpf.12618

ORIGINAL ARTICLE

WILEY Clinical Physiology and Functional Imaging

Threshold-automated CT measurements of muscle size and radiological attenuation in multiple lower-extremity muscles of older individuals

Hans E. Berg[1,2] | Daniel Truong[1,2] | Elisabeth Skoglund[3,4,5] | Thomas Gustafsson[4,5] | Tommy R. Lundberg[4,5]

[1]Department of Clinical Science, Intervention and Technology, Karolinska Institutet, Stockholm, Sweden

[2]Department of Orthopaedic Surgery, Karolinska University Hospital, Stockholm, Sweden

[3]Department of Public Health and Caring Sciences, Clinical Nutrition and Metabolism, Uppsala University, Uppsala, Sweden

[4]Division of Clinical Physiology, Department of Laboratory Medicine, Karolinska Institutet, Stockholm, Sweden

[5]Unit of Clinical Physiology, Karolinska University Hospital, Stockholm, Sweden

Correspondence
Hans E. Berg, Department of Orthopaedic Surgery, Karolinska University Hospital, Hälsovägen, SE-14186 Stockholm, Sweden.
Email: hans.berg@ki.se

Funding information
Stockholms Läns Landsting, Grant/Award Number: ALF/SLL20150168, ALF/SLL20180498; Medicinska Forskningsrådet, Grant/Award Number: 2013-09305; Nestlé Health Science, Grant/Award Number: CTA# 10.27.CLI; CIMED, Grant/Award Number: 20180831

Abstract

Muscle atrophy and fat infiltration, two indicators of deconditioning and weakness in elderly frail patients, are typically assessed by means of manual image analysis from computed tomography (CT) scans. As this time-consuming image analysis limits its wider use in clinical studies, the use of tissue thresholds to semi-automatically assess muscle composition has been suggested. Here, we aimed to investigate the relationship between manual and semi-automated analysis of both cross-sectional area (CSA) and radiological attenuation (RA), in multiple muscles of the lower extremities in aged (77 ± 6 years) sedentary individuals (n = 40). The participants underwent CT scans of their lower limbs, including hip, thigh and calf muscles. The subsequent analysis of CSA and RA was conducted using both manual segmentation and semi-automatic thresholds (−30 to +150 Hounsfield units). Automated measurements were generally strongly correlated with manually encircled CSA in all muscle groups (R = 0.79–0.99, $p < .05$) and shortened the analysis time by 70% ($p < .05$). In m. iliopsoas, however, the CSA became overestimated (15%, $p < .05$) with thresholded measurements, while the assessment of both CSA and RA was underestimated in muscles with high-fat content (i.e., the gluteal muscles) and in individuals with high-fat infiltration. In conclusion, using the semi-automated technique with conventional thresholds is a time-saving method that delivers accurate gross size of the muscle groups, particularly in the thigh. However, caution should be exercised when using semi-automated techniques for assessing CSA and fat infiltration in muscles with high-fat content.

KEYWORDS

computed tomography, fat infiltration, hounsfield units, muscle atrophy, sarcopenia, skeletal muscle

1 | INTRODUCTION

Computed tomography (CT) using X-rays opened up the field of medical imaging and allowed for characterization of organs inside the human body (Hounsfield, 1973). Since muscle function is closely related to the cross-sectional area (CSA) and volume of a given muscle, tomographic imaging has remained central to quantify muscle hypertrophy in response to training (Narici, Roi, & Landoni, 1988) or atrophy in response to inactivity (Berg, Eiken, Miklavcic, & Mekjavic, 2007) and disease (Goodpaster, Thaete, & Kelley, 2000). Furthermore, radiological attenuation (RA), assessed in Hounsfield units (HU), is a sensitive marker of fatty infiltration when using CT to monitor muscles of aged, deconditioned or inactive individuals (Berg, Dudley, & Haggmark, 1991; Goodpaster et al., 2000; Grindrod, Tofts, & Edwards, 1983; Rasch, Byström, Dalen, & Berg, 2007). Indeed, increased fat infiltration is seen in, for example, osteoarthritic and sarcopenic individuals (Narici, Franchi, & Maganaris, 2016; Rasch et al., 2007) and is generally associated with several comorbidities (Cruz-Jentoft, Bahat, & Bauer, 2018), highlighting the clinical relevance of this measure.

Although the classic routine of manually circumscribing individual muscles in tomographic images allows for simultaneous assessment of both CSA and RA of any muscle group, manual assessment is highly time-consuming, which limits its use in large clinical studies. Furthermore, delineating each muscle belly manually demands substantial anatomical skill of the operator and may thus lead to errors and poor inter-rater reproducibility of measurements. Attempts to address these issues, enabled by computer and software development, include partial automatization of CSA or volume measurements (Irving, Weltman, & Brock, 2007; Strandberg, Wretling, Wredmark, & Shalabi, 2010) using preset thresholds for what constitutes fat versus muscle tissue.

The use of attenuation thresholds can be considered for at least two reasons. First, it can be used when the aim is to detect a specific tissue of interest (i.e., muscle) for biologic study, while excluding other tissues (i.e., fat or bone). A second more pragmatic reason is to optimize the measurement technique in order to save substantial analysis time. Since many studies have a preset time budget, this could translate into more muscle groups or more subjects being assessed within a specific research project. The above two factors could in fact act in synergy, and some researchers apply threshold segmentation to obtain fat-free, or contractile, muscle area in a single step (Strandberg et al. 2010). Conversely, many studies employing magnetic resonance imaging (MRI) or ultrasonography simply report total CSA as the muscle size, neglecting that the non-contractile portion of the muscle may vary substantially (Franchi, Longo, & Mallinson, 2018).

A complicating factor to consider is, however, that the optimal lower and upper HU-threshold values to define contractile muscle are still under debate (Dube et al. 2011, Aubrey, Esfandiari, & Baracos, 2014). It is therefore uncertain whether semi-automated measurements could replace the manual method when assessing muscle CSA and composition in CT images. Moreover, given that previous studies mainly have analysed muscles of the thigh or the trunk, data from multiple lower-limb muscles are currently lacking. Therefore, the objective of this study was to investigate the relationship between manual and semi-automated techniques, in terms of their ability to deliver assessments of both CSA and RA, in multiple muscles of the lower extremities in aged individuals. Because fat content, and thereby RA, varies substantially between different muscles, we hypothesized that CSA and RA measurements would show different degrees of measurement errors depending on the specific lower-limb muscle being analysed. We also hypothesized that the time consumption for image analysis would be markedly shortened by employing semi-automated measurements.

2 | METHODS

2.1 | Subjects

The CT scans were from the Swedish cohort of 66 patients who had completed a clinical trial investigating the effects of exercise and nutrition on muscle mass and performance (Kirn, Koochek, & Reid, 2015). At the time of the current analysis, we had access to and analysed 19 women and 21 men (n = 40, age 77 ± 6 years, body mass 80 ± 14 kg, height 169 ± 9 cm). From these subjects, 39 scans were analysed for thigh and calf muscles and 36 individuals for hip muscles (some images could not be analysed due to exporting failure). Inclusion criteria for the clinical trial were as follows: community dwelling men or women aged 70 years or more who were capable of walking 400 m within 15 min, had a body mass index of 35 or less, a score in the Short Physical Performance Battery of <9, and a mini mental state ≥ 24. They were all low in Vitamin D levels, Serum-25-(OH)-D in the range of 22.5–60 nM. Exclusion criteria and further details are described in the VIVE2 study protocol (Kirn et al., 2015). Permission by the regional ethical review board in Stockholm (Dnr: 2012/154) was obtained for the VIVE2 study including the performance of all CT scans.

2.2 | CT protocol

Muscle CSA (mm^2) and RA (HU) were assessed in multiple transaxial images on three levels in both lower limbs (left/right): hips, thighs and calves, using 5 mm slice thickness obtained by a spiral CT scanner (General Electric Medical Systems) operating at 120 kV, 100 mAs with a 1.5-s scan time. Subjects were scanned following 30–60 min of bed rest in order to minimize the influence of postural fluid shifts on muscle size (Berg, Tedner, & Tesch, 1993). Limb rotation was standardized using a strap around the feet. Anatomical landmarks were used to accurately target the same area in all subjects.

2.3 | Image analysis

Image series for hip muscles were selected a few centimetres proximal to the femoral head. Two DICOM images for each individual were selected at the lower end of the sacroiliac joint; at the vertex of the greater sciatic foramen. Thigh images were selected 200 mm

proximal to the knee joint space, by the lateral apex of the femur condyle. Calf images were selected 130 mm distal to the same point at the knee joint space, corresponding roughly to the maximum girth of the calf (Berg et al., 2007) NIH ImageJ (Bethesda, MD) was used to analyse all DICOM formatted images on a standard HD computer screen. Anatomical CSA and RA were automatically calculated and stored in spreadsheets.

The ID of patients was obscured in all images, and encrypted codes without ID were used. Each patient was assessed for CSA and RA using one manual method and one semi-automatic method. The same observer performed all the measurements in a blinded manner. However, in order to assess the inter-rater reliability for the manual analysis, the muscle groups were also manually segmented by a second observer with similar prior experience of CT segmentation. A total of eight muscle groups were measured in each lower limb: gluteus minimus/medius (principal hip abductors), gluteus maximus (prinicipal hip extensor), iliopsoas (hip flexor), quadriceps femoris (knee extensor), hamstrings (knee flexors), hip adductors, posterior calf muscles (ankle plantar flexors) and anterior calf muscles (ankle dorsiflexors).

2.3.1 | Manual measurement

The classic method of manually circumscribing each muscle for muscle CSA and RA was used (Aubrey et al., 2014; Rasch et al., 2007). The region of interest (ROI) was identified, and then, the muscle borders were encircled using the polygon tool in ImageJ, and care was taken to avoid low-attenuating fat or high-attenuating bone (Figure 1).

2.3.2 | Semi-automated measurement using thresholds

Set thresholds for tissue attenuation aimed to exclude any non-muscular tissue in the ROI. The range of −29 HU to +150 HU was chosen to include low-attenuation muscle, which may constitute more than 10% of the whole muscle (Aubrey et al., 2014). Hence, a filter emerged on the image, clearly visualizing tissues included within the threshold limits (Figure 1). Then, a rough ROI encircling actual muscle tissues was drawn, and CSA and RA within the chosen thresholds were automatically computed. This process was repeated for each muscle or muscle group. In both methods, a second image of the same area was open as a guide map while the other image was being measured.

2.3.3 | Time to rate

To evaluate potential differences in time consumption between the manual and semi-automated method, a standardized measurement of two image sets of hip muscles (three muscles on left and right sides, respectively; a total of 12 measurements for each participant) was timed. For the manual measurement, the timer started when both images had been opened and was stopped when the last measurement had been completed. For semi-automated measurements, the timer started when the two images were opened, but before applying the threshold filter, as this is a mandatory additional step compared to the manual measurement.

2.4 | Data analysis

The relationship between manual and thresholded segmentation of muscle area and radiological density was assessed using linear regression (Pearson's *r*-value). Further, the systematic and random errors (mean bias and 95% limits of agreement) were assessed using Bland–Altman graphs. The difference in mean values between the two methods (systematic bias) and the two legs was assessed for each muscle group using a two-way ANOVA with factors method (MAN vs. AUT) and leg (Left vs. Right). An alpha-level of 5% was accepted as significant for all statistical analyses.

The two-way ANOVA was conducted using SPSS v. 24 (Chicago, IL). All of the other variables were computed in GraphPad Prism 7 (GraphPad Software Inc, Cal). In addition, the inter-rater reliability was computed using the spreadsheets provided at sportsci.org (sportsci.org/2015/ValidRely.htm). Each leg was treated as an independent observation.

3 | RESULTS

The mean time to rate was 1,174 (*SD* = 252) and 370 (*SD* = 64) seconds for manual and semi-automated measurements, respectively.

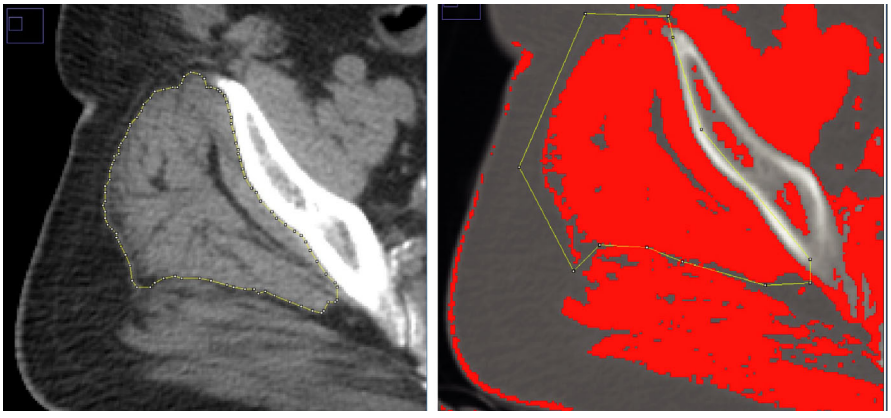

FIGURE 1 Example images of the manual versus thresholded technique to encircle muscle bellies, in this case the gluteus medius and minimus. In the manual method, the targeted muscle is segmented carefully just underneath the muscle fascia and outside the bone. In the threshold-segmenting method, gross division well outside muscle is performed. The coloured pixels denoted the contractile tissue (i.e., the pixels that fall within the preset threshold for muscle)

Thus, the threshold technique was approximately 3.2 times faster ($p < .01$) than the manual method.

The mean area and attenuation of the different muscle groups and limbs, assessed with manual and thresholded segmentation, are displayed in Table 1. There were significant systematic differences between the two methods for most of the muscle groups. For CSA, four out of eight muscle groups reached statistical significance, where all muscle groups except the iliopsoas and ankle dorsiflexors differed less than 5%. For the RA analysis, all muscle groups except the plantar- and dorsiflexors showed a statistically significant bias between methods, although only the gluteus min/medius differed more than five HU. For most of the muscle groups, there were no baseline differences in muscle area or attenuation between the right and left limb muscles. Exceptions were RA of the gluteus maximus, where left limb had 2.8 HU greater value and CSAs of the ankle dorsiflexors (right limb had 4% greater area).

The correlation analysis and Bland–Altman blots, with corresponding data (*R*-values, bias and 95% limits of agreement) are shown in Figures 2 and 3 for the thigh, hip and calf muscles, and for CSA and RD, respectively. In general, the correlations between manual and thresholded segmentation showed high *r*-values (all $r > 0.9$ except CSA of gluteus min–medius and maximus. However, the random error (estimated from the 95% limits of agreement) was rather high for several of the muscle groups. Finally, Figure 4 shows the bias in thresholded RA as a function of the HU attenuation value and the bias in CSA at different levels of RA.

For the inter-rater reliability analysis of manual segmentation, the *r*-value, intra-class correlation, mean bias and typical error for CSA and RA are summarized in Table 2. Generally, there were high correlations between the two independent observers. However, the typical error still exceeded 5% for several of the muscle groups.

4 | DISCUSSION

Reduced muscle size and increased fat infiltration are clinical hallmarks of muscle deconditioning. In the current study, we applied and compared the two commonly employed techniques for measuring CSA and RA, in multiple lower-limb muscles. The excellent correlation between semi-automated and manual assessment of CSA in low-fat muscles and more than fair correlation in all muscles was one of the main findings of this study. There was, however, a substantial mismatch between total and threshold-segmented CSA of the iliopsoas muscle, as well as in individuals with fat-rich muscles. Likewise, a systemic bias in RA when using automated measurement in fat-rich muscles occurred, which must be considered when using threshold segmentation techniques.

The correlation between CSA values assessed by manual and semi-automated techniques was high for most muscle groups and very high in the thigh (knee extensors, knee flexors and hip adductors), while moderate in the gluteal muscles of the hip. The overall bias in CSA between methods was modest, yet increased in muscles generally rich in fat. Thus, CSA of gluteus minimus/medius, adductors in the thigh, and dorsal calf muscles was slightly underestimated

TABLE 1 Cross-sectional area (mm^2) and radiological attenuation (RA; Hounsfield units) of all examined muscle groups (right and left) with method (manual or threshold-segmented) bias in % or Hounsfield units (HU) and their statistical *p*-values

		Cross-sectional area				Radiological attenuation			
		Method data (mm^2)		Method	Method bias	Method data (HU)		Method	Method bias
Muscle group		Manual	Thresholded	Bias Δ%	*p*-Value	Manual	Thresholded	Bias ΔHU	*p*-Value
Knee extensors	Right	4,433 (1,057)	4,461 (1,050)	0.8	.065	47.8 (7.5)	49.8 (6.5)	2.0	<.0001
	Left	4,426 (996)	4,472 (1,048)			48.0 (7.4)	49.6 (6.4)		
Knee flexors	Right	2,726 (718)	2,742 (699)	0.6	.400	35.2 (10.5)	36.2 (8.4)	1.0	.009
	Left	2,725 (646)	2,743 (638)			36.1 (12.2)	37.4 (9.6)		
Hip adductors	Right	2,027 (675)	2,005 (658)	−1.7	.014	36.6 (9.2)	38.9 (7.0)	2.3	<.0001
	Left	2,036 (703)	1,986 (694)			37.9 (9.4)	40.1 (7.7)		
Gluteus min/medius	Right	4,130 (704)	3,927 (714)	−3.8	.034	25.2 (15.8)	34.0 (8.6)	8.8	<.0001
	Left	4,123 (633)	4,011 (713)			27.6 (15.4)	35.2 (8.7)		
Gluteus maximus	Right	3,186 (770)	3,232 (732)	1.7	.317	19.8 (13.3)	21.7 (10.0)	1.9	.021
	Left	3,207 (656)	3,269 (633)			23.3 (14.2)	24.5 (11.1)		
Iliopsoas	Right	1,294 (369)	1,491 (392)	15.1	<.0001	53.5 (6.0)	52.9 (4.9)	−0.6	.006
	Left	1,287 (364)	1,481 (368)			54.8 (6.0)	53.3 (5.2)		
Ankle dorsiflexors	Right	1,705 (335)	1,792 (383)	5.3	<.0001	45.2 (12.1)	46.7 (9.9)	1.5	.055
	Left	1,645 (306)	1,736 (328)			45.6 (12.8)	46.3 (9.9)		
Ankle plantar flexors	Right	4,146 (1,088)	4,150 (1,014)	0.4	.824	43.5 (13.7)	45.1 (9.5)	1.6	.084
	Left	4,151 (1,144)	4,179 (1,173)			45.0 (14.6)	46.0 (10.5)		

Note. Data are means (*SD*). Method bias *p*-values denote ANOVA main effect comparisons.

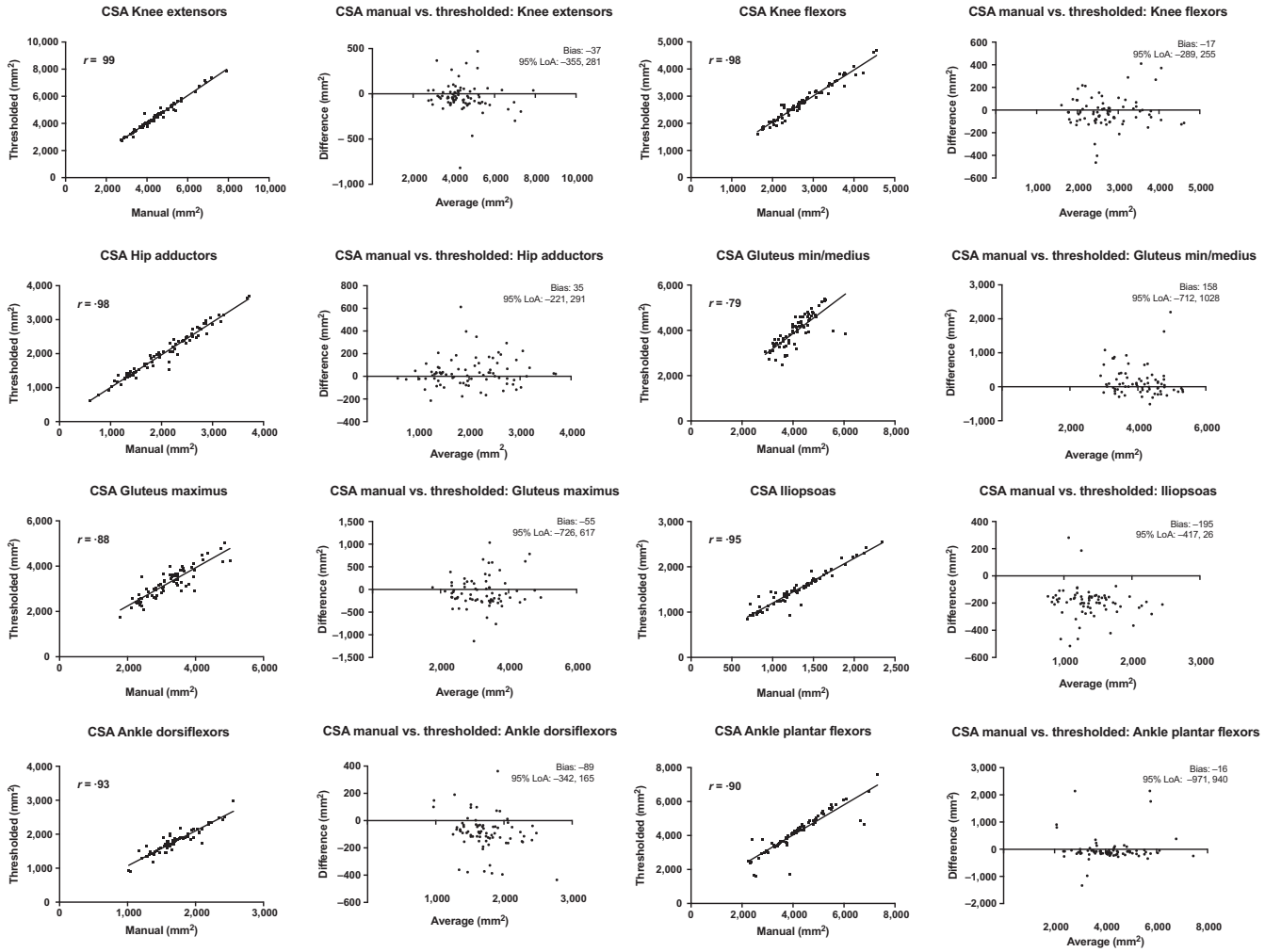

FIGURE 2 Pairs of graphs for the eight measured muscle groups. The left graph shows the linear correlation between automated and the thresholded cross-sectional area (CSA) measurements. The right graph shows the Bland–Altman plot with associated bias and 95% limits of agreement (LoA). Values are in mm^2

(2%–4%) when using the semi-automated threshold method (Table 1). When this bias was expressed as a function of the HU attenuation value (Figure 4d), it seems clear that individuals with muscles rich in fat show gross discrepancies when using threshold-segmented CSA. In contrast, and more encouraging, our results show that in individuals with muscles containing a modest amount of fat (RA 30–60 HU), thresholded and manual measurements show excellent agreement. This indicates that muscles of healthy and young individuals, and also muscle groups with an overall low-fat content (e.g., the knee extensors), could be monitored interchangeably with either the manual or thresholded method. Conversely, individuals having large amounts of intramuscular fat, and potentially any muscle being rich in fat (i.e., the gluteal muscles), need careful methodological adjustment before an automated threshold technique can be considered.

Reduced RA of whole muscle, as an index of fatty infiltration, has been associated with metabolic dysfunction, frailty and even risk of falls (Goodpaster et al., 2000). Yet, when using thresholded segmentation methods to measure muscle size, information of RA is typically not reported. Our results show that correlations in RA between methods were very high in almost all lower-limb muscles. However, there was a consistent bias in RA values between the manual and thresholded method, which grew linearly with increased fat content as indicated by decreasing RA (Figures 3and4). This bias in fattier muscles is actually expected since manual measurements deliver the true average of all picture elements (pixels) of an encircled area, while automated threshold-segmented RA includes only pixels already predefined as skeletal muscle tissue. Thus, information on the true composition of the muscle is therefore lost when using the predefined conventional thresholds. Consequently, with the exception of the relatively lean iliopsoas and knee flexors, RA was overestimated by 1.5–8 HU when using threshold segmentation compared to manual assessment, and differences exceeding 20 HU were manifested in fat-rich muscles at the low end of the spectrum. Altogether, it seems that assessment of RA should be interpreted with caution when semi-automated threshold techniques have been used. Future studies need to clarify the relevance of threshold-segmented RA values, especially in fat-rich muscles and if they are representative or reliable for lean muscles, such as in young and healthy

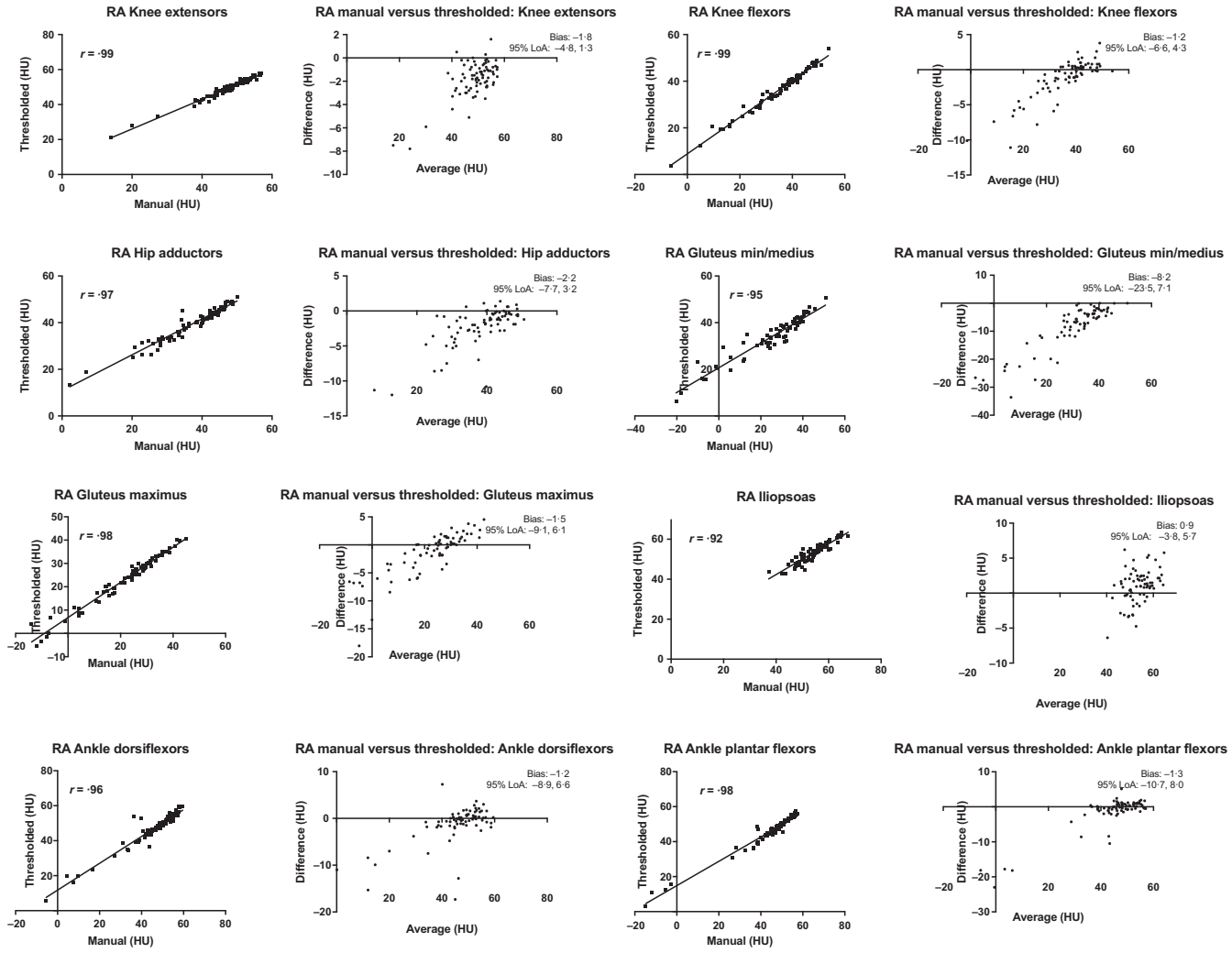

FIGURE 3 Pairs of graphs for the eight measured muscle groups. The left graph shows the linear correlation between automated and the thresholded radiological attenuation (RA) measurements. The right graph shows the Bland–Altman plot with associated bias and 95% limits of agreement (LoA). Values are in Hounsfield units (HU)

individuals. Also, the question if threshold-segmented RA, despite bias, could accurately trace changes secondary to interventions or maladies, needs to be explored.

An advantage with automated measurements using RA thresholds is that it may reduce the influence of the human factor and, thus, reduce the need of skilled raters while still reducing analysis time. Indeed, our inter-rater analysis indicated that subtle differences in anatomical decisions influence the reliability of the manual measurements. Tracing the muscle borders automatically is therefore desirable and has recently been described for the thigh muscles using MRI (Karlsson, Rosander, & Romu, 2015; Thomas, Newman, & Leinhard, 2014). Still, however, there is no fully automated technique described for CSA or volume quantification of individual muscles using CT. Individual muscle groups have been measured semi-automatically by roughly creating the outer border allowing for automatic segmentation of the enclosed area (Steiger, Block, & Friedlander, 1988). Similarly, we used an initial muscle segmentation to highlight outer borders and added division lines to bony landmarks in order to obtain a time-efficient strategy when creating the outer boundary of a specific muscle. The highly reduced examination time would allow for a threefold increase in investigated muscle areas per session, supporting the use of the thresholded method whenever feasible.

Although previous data are lacking, we worried that irregular, less homogenous and smaller muscles would be more vulnerable to methodological errors both in terms of CSA and RA. While most muscles showed excellent correlations across techniques, which are reassuring for future CT studies of multiple muscle groups, there was indeed a marked method difference in the CSA assessment of the iliopsoas muscle, one of the smallest muscles. A careful examination of these measurements revealed that this was likely due the operator delineating the muscle borders with an exaggerated safety distance to the muscle fascia in order not to enclose non-muscular tissue. The variation between techniques seems to increase with smaller iliopsoas size (Figure 2), while no marked bias is apparent in the larger muscles. Also, there was a large method bias in RA when using threshold segmentation of the gluteus medius and minimus

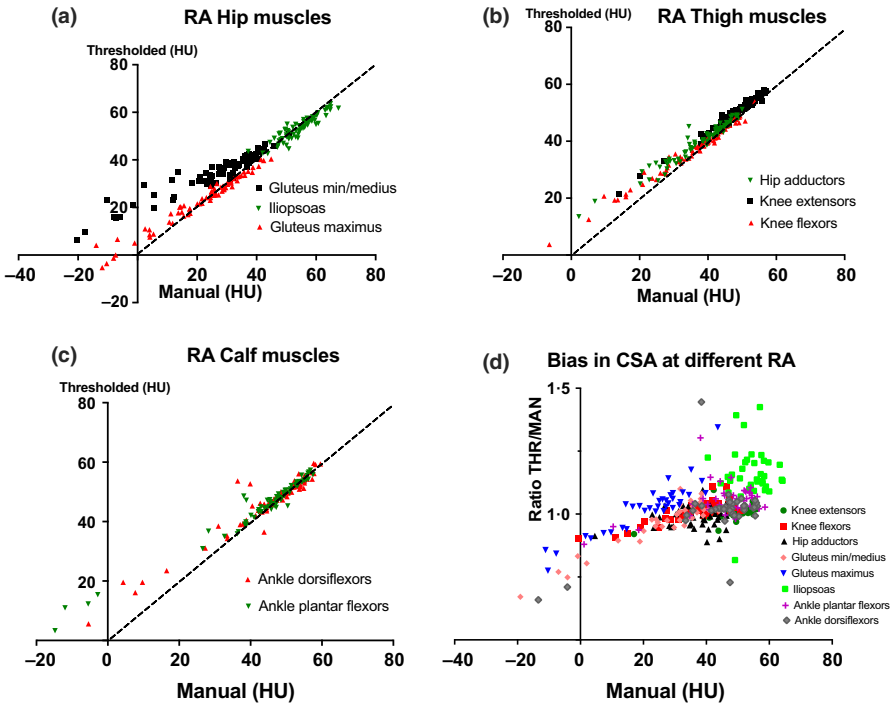

FIGURE 4 Graphs per region. (a) hip (gluteus maximus, min/medius, iliopsoas), (b) thigh (knee extensors, flexors, hip adductors) or (c) calf (ankle plantar flexors, dorsiflexors) muscles, are displayed by their automated radiological attenuation (RA) (in HU; *y*-axis) as a function of their manually assessed RA (*x*-axis). Graph (d) shows all muscle groups by their bias in CSA (ratio automated/manual; *y*-axis) as a function of their RA (in HU; *x*-axis). Ratio 1.0 denotes equal automated and manually measured CSA

TABLE 2 Inter-rater bias, typical error, *r*-value and intra-class correlation (ICC)

	Cross-sectional area				Radiological attenuation			
Muscle group	Mean bias (%)	Typical error (mm^2)	*r*-Value	ICC	Mean bias (HU)	Typical error (HU)	*r*-Value	ICC
Knee extensors	5.7	110	.99	0.99	3.8	0.2	.98	0.98
Knee flexors	3.9	183	.93	0.92	4.0	1.8	.98	0.98
Hip adductors	6.0	211	.91	0.91	0.8	1.5	.97	0.97
Gluteus min/medius	4.0	371	.76	0.75	2.6	2.1	.98	0.98
Gluteus maximus	5.3	188	.94	0.94	3.4	1.2	.99	0.99
Iliopsoas	4.3	106	.92	0.92	3.6	2.3	.85	0.86
Ankle dorsiflexors	5.8	95	.93	0.92	1.7	4.0	.91	0.90
Ankle plantar flexors	2.7	120	.99	0.99	3.3	1.2	.99	0.99

Abbreviation: HU, Hounsfield units.

muscles, particularly when compared to the adjacent gluteus maximus muscle, expressing similar RA and indicating gross fatty infiltration. While the reason for this finding is not clear, it was observed that the gluteus medius and minimus group, similar to the plantar flexors of the ankle, exhibit macroscopic extramuscular fat patches larger than the image pixel size. These would be excluded during thresholded segmentation, but not easily excluded with the manual measurement. Thus, future studies should investigate if threshold-segmented techniques could be adapted to the morphology or geometry of the specific muscles being assessed.

The investigation of multiple lower-limb muscle groups, heterogenous in size and RA, and the large group of individuals was a strength of the current study. A limitation was that we only examined a homogenous group of sedentary older individuals, and therefore, the findings are not readily valid for young, highly aged or metabolically deranged individuals. However, the wide variation in muscular fat and size between the large number of individuals might in part have counteracted this limitation. Future studies should examine other fat-rich muscles, including muscle composition of obese individuals, and the accuracy of the semi-automated technique when assessing longitudinal changes in response to interventions or disease. Finally, a finding worth to recognize was that there were generally non-significant differences between right and left limbs, suggesting that only one limb needs to be measured to follow an intervention, while the contra-lateral limb could be used for comparison within unilateral interventions or in disease and/or injury.

In conclusion, we report strong correlations between semi-automated and manual assessment of CSA, particularly in low-fat muscles. Thus, using conventional thresholds (−30 to +150 HU) with the semi-automated technique is a time-saving method that delivers accurate gross size (CSA) of the muscle groups in the thigh. However, caution should be exercised with measurements

of CSA and RA in fattier muscles, as illustrated by the gluteal and calf muscles in our sedentary patient cohort.

ACKNOWLEDGMENTS

The CT images in this work came from the Swedish cohort included in the VIVE2 study, which was supported by Nestlé Health Science, Vevey, Switzerland (CTA# 10.27.CLI). HEB was supported by grants within the Stockholm regional clinical research agreement (ALF/SLL20150168, ALF/SLL20180498, CIMED/SLL20180831). TG was supported by a grant from the Swedish Medical Research Council (2013-09305). The radiological expertise and guidance of Associate Professor Torkel Brismar at the Karolinska Institutet and Karolinska University Hospital is greatly acknowledged. Dr. Afsaneh Koochek and Dr. Åsa von Berens are acknowledged for their work as coordinators of the primary study.

CONFLICT OF INTEREST

The authors declare that they have no conflict of interest.

ORCID

Tommy R. Lundberg https://orcid.org/0000-0002-6818-6230

REFERENCES

Aubrey, J., Esfandiari, N., Baracos, V. E., Buteau, F. A., Frenette, J., Putman, C. T., & Mazurak, V. C. (2014). Measurement of skeletal muscle radiation attenuation and basis of its biological variation. *Acta Physiologica*, *210*, 489–497. https://doi.org/10.1111/apha.12224

Berg, H. E., Dudley, G. A., Haggmark, T., Ohlsen, H., & Tesch, P. A. (1991). Effects of lower limb unloading on skeletal muscle mass and function in humans. *Journal of Applied Physiology*, *70*, 1882–1885. https://doi.org/10.1152/jappl.1991.70.4.1882

Berg, H. E., Eiken, O., Miklavcic, L., & Mekjavic. I. B. (2007). Hip, thigh and calf muscle atrophy and bone loss after 5-week bedrest inactivity. *European Journal of Applied Physiology*, *99*, 283–289. https://doi.org/10.1007/s00421-006-0346-y

Berg, H. E., Tedner, B., Tesch, P. A. (1993). Changes in lower limb muscle cross-sectional area and tissue fluid volume after transition from standing to supine. *Acta Physiologica Scandinavica*, *148*, 379–385. https://doi.org/10.1111/j.1748-1716.1993.tb09573.x

Cruz-Jentoft, A. J., Bahat, G., Bauer, J., Boirie, Y., Bruyere, O., Cederholm, T., … Schols J. (2018). Sarcopenia: Revised European consensus on definition and diagnosis. *Age and Ageing*, *48*, 16–31. https://doi.org/10.1093/ageing/afy169.

Dubé, J. J., Amati, F, Toledo, F. G. S., Stefanovic-Racic, M., Rossi, A., Coen, P., & Goodpaster, B. H. (2011). Effects of weight loss and exercise on insulin resistance, and intramyocellular triacylglycerol, diacylglycerol and ceramide. *Diabetologia*, *54*, 1147–1156. https://doi.org/10.1007/s00125-011-2065-0

Franchi, M. V., Longo, S., Mallinson, J., Quinlan, J. I., Taylor, T., Greenhaff, P. l., & Narici, M. V. (2018). Muscle thickness correlates to muscle cross-sectional area in the assessment of strength training-induced hypertrophy. *Scandinavian Journal of Medicine & Science in Sports*, *28*, 846–853. https://doi.org/10.1111/sms.12961

Goodpaster, B. H., Thaete, F. L., Kelley, D. E. (2000). Composition of skeletal muscle evaluated with computed tomography. *Annals of the New York Academy of Sciences*, *904*, 18–24. https://doi.org/10.1111/j.1749-6632.2000.tb06416.x

Grindrod, S., Tofts, P., Edwards, R. (1983). Investigation of human skeletal muscle structure and composition by X-ray computerised tomography. *European Journal of Clinical Investigation*, *13*, 465–468. https://doi.org/10.1111/j.1365-2362.1983.tb00130.x.

Hounsfield, G. N. (1973). Computerized transverse axial scanning (tomography): I. Description of system. *British Journal of Radiology* ,*68*, H166–H172.

Irving, B. A., Weltman, J. Y., Brock, D. W., Davis, C. K., Gaesser, G. A., & Weltman, A. (2007). NIH ImageJ and Slice-O-Matic computed tomography imaging software to quantify soft tissue. *Obesity*, *15*, 370–376. https://doi.org/10.1038/oby.2007.573

Karlsson, A., Rosander, J., Romu, T., Tallberg, J., Grönqvist, A., Borga, M, & Dahlqvist Leinhard, O. (2015). Automatic and quantitative assessment of regional muscle volume by multi-atlas segmentation using whole-body water-fat MRI. *Journal of Magnetic Resonance Imaging*, *41*, 1558–1569. https://doi.org/10.1002/jmri.24726

Kirn, D. R., Koochek, A., Reid, K. F., von Berens, Å., Travison, T. G., Folta, S., … Fielding, R. A. (2015). The Vitality, Independence, and Vigor in the Elderly 2 Study (VIVE2): Design and methods. *Contemporary Clinical Trials*, *43*, 164–171. https://doi.org/10.1016/j.cct.2015.06.001

Narici, M., Franchi, M., Maganaris, C. (2016) Muscle structural assembly and functional consequences. *Journal of Experimental Biology*, *219*, 276–284. https://doi.org/10.1242/jeb.128017

Narici, M. V., Roi, G. S., & Landoni, L. (1988). Force of knee extensor and flexor muscles and cross-sectional area determined by nuclear magnetic resonance imaging. *European Journal of Applied Physiology and Occupational Physiology*, *57*, 39–44. https://doi.org/10.1007/BF00691235

Rasch, A., Byström, A. H., Dalen, N., & Berg, H. E. (2007). Reduced muscle radiological density, cross-sectional area, and strength of major hip and knee muscles in 22 patients with hip osteoarthritis. *Acta Orthopaedica*, *78*, 505–510. https://doi.org/10.1080/17453670710014158

Steiger, P., Block, J. E., Friedlander, A., Genant, H. K. (1988). Precise determination of paraspinous musculature by quantitative CT. *Journal of Computer Assisted Tomography*, *12*, 616–620. https://doi.org/10.1097/00004728-198807000-00015.

Strandberg, S., Wretling, M.-L., Wredmark, T., & Shalabi, A. (2010). Reliability of computed tomography measurements in assessment of thigh muscle cross-sectional area and attenuation. *BMC Medical Imaging*, *10*, 18. https://doi.org/10.1186/1471-2342-10-18

Thomas, M. S., Newman, D., Leinhard, O. D., Kasmai, B., Greenwood, R., Malcolm, P. N., … Toms, A. P. (2014). Test-retest reliability of automated whole body and compartmental muscle volume measurements on a wide bore 3T MR system. *European Radiology*, *24*, 2279–2291. https://doi.org/10.1007/s00330-014-3226-6

How to cite this article: Berg HE, Truong D, Skoglund E, Gustafsson T, Lundberg TR. Threshold-automated CT measurements of muscle size and radiological attenuation in multiple lower-extremity muscles of older individuals *Clin Physiol Funct Imaging*. 2020;40:165–172. https://doi.org/10.1111/cpf.12618